molecular pharmaceutics

Article

pubs.acs.org/molecularpharmaceutics

Mechanistic Studies of the Effect of Bile Salts on Rhodamine 123 Uptake into RBE4 Cells

Lin Yang,*[,†] J. Paul Fawcett,[†] Jesper Østergaard,[‡] Hu Zhang,[†] and Ian G. Tucker[†]

[†]School of Pharmacy, University of Otago, Dunedin, New Zealand

[‡]Department of Pharmaceutics and Analytical Chemistry, Faculty of Pharmaceutical Sciences, University of Copenhagen, Universitetsparken 2, 2100 Copenhagen, Denmark

ABSTRACT: To examine the ability of bile salts (BS) to act as permeation enhancers at the blood brain barrier, the effect of four BS (cholate, deoxycholate, monoketocholate and taurocholate) on accumulation of rhodamine 123 (R123) in rat brain endothelial (RBE4) cells was investigated. Experiments were performed using BS concentrations shown to be noncytotoxic to RBE4 cells. Uptake and efflux of R123 in the absence and presence of BS were studied by fluorescence spectroscopy and confocal microscopy. Changes in RBE4 cell membrane fluidity in the presence of BS were evaluated using fluorescence anisotropy. The direct interaction between BS and R123 (ion pairing) and the effect of BS on distribution of R123 into liposomes were studied by capillary electrophoresis. All BS influenced R123 uptake in a concentration-dependent manner and increased cell membrane fluidity. Monoketocholate produced the greatest increase in uptake and also significantly reduced R123 efflux probably by inhibition of P-glycoprotein (P-gp). Direct interaction of BS and R123 was weak, but distribution of R123 into liposomes was increased by BS. The results suggest that BS increase R123 uptake by increasing cell membrane fluidity and, in the case of MKC, by inhibiting P-gp.

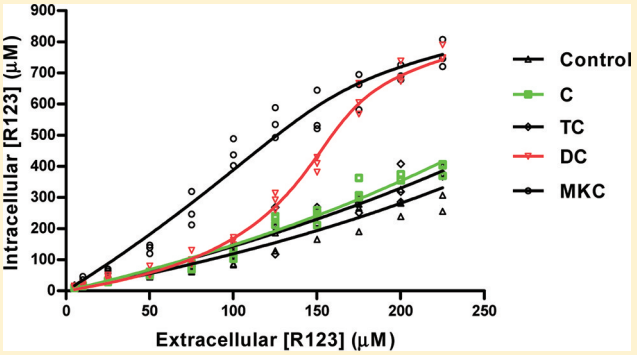

KEYWORDS: *blood brain barrier, bile salts, rhodamine 123, RBE4 cells*

INTRODUCTION

The combination of tight junctions, an endothelial cell membrane with high lateral packing density and the expression of efflux transporters severely limits drug transport across the blood brain barrier (BBB). Bile salts (BS) have been widely studied as permeation enhancers to increase drug transport across various biological barriers, but studies of their effect on the BBB are limited. BS have been shown to facilitate drug transport via both paracellular and transcellular pathways,[1,2] but their ability to affect these pathways at the BBB is unknown.

A novel semisynthetic BS, 12-monoketocholate (MKC), has been shown to increase drug uptake into the brain,[3−5] but it is not clear whether this is a class effect of BS or specific to MKC. Certainly the keto group at position 12 in MKC makes it significantly less surface active and less lipophilic than cholate (C) and consequently less toxic.[6] Previously, we investigated the effects of C, MKC, deoxycholate (DC) and taurocholate (TC) on the transport of the hydrophilic drug morphine-6-glucuronide (M6G) across RBE4 cell monolayers.[7] It was found that, at high concentrations (2−5 mM), BS increased the paracellular permeation of M6G in this model of the BBB.

In this paper we report an investigation of the effect of C, MKC, DC and TC on the uptake and efflux of rhodamine 123 (R123) in RBE4 cells to elucidate how BS affect transcellular transport across the BBB. R123 is a cationic, hydrophobic compound (clogP 2.85) and well-known P-glycoprotein (P-gp) substrate.[8] Uptake of R123 into cells has generally been assumed to involve passive diffusion[9] limited by efficient efflux by P-gp.[10] The mechanism of the effect of BS was investigated through equilibrium uptake studies and mathematical modeling thereof, and by measuring efflux of R123 from preloaded cells. These data were supported by assessment of the effect of the four BS on RBE4 cell membrane fluidity and the liposome/buffer distribution coefficient of R123 as well as by assessment of BS-R123 ion pair formation. The overall aim of the study was to provide a solid basis for further investigations into the use of BS to enhance drug delivery to the brain.

METHOD

Materials. MKC was a gift from Professor Ksenija Kuhajda (University of Novi Sad, Serbia). C, DC, TC, Ringer's buffer (10 mM D-glucose; 0.23 mM $MgCl_2$; 0.45 mM KCl; 120 mM NaCl; 0.70 mM Na_2HPO_4; 1.5 mM NaH_2PO_4), HEPES, calcium chloride, sodium bicarbonate, sodium dodecyl sulfate (SDS) 1,2-dipalmitoyl-*sn*-glycero-3-phosphocholine (DPPC), 1,6-diphenyl-1,3,5-hexatriene (DPH), 1-(4-trimethylammoniumphenyl)-6-phenyl-1,3,5-hexatriene (TMA-DPH), tetrahydrofuran (THF), DMSO, Triton X-100 and R123 were purchased from

Received: April 17, 2011
Revised: September 24, 2011
Accepted: November 3, 2011
Published: November 3, 2011

Sigma-Aldrich (Auckland, NZ). Dulbecco's modified Eagle's medium (DMEM), minimum essential medium (alpha medium), F-10 Nutrient Mixture, Hanks balanced salt solution (HBSS), fetal bovine serum (FBS), trypsin-EDTA, penicillin–streptomycin, Geneticin and glutamine were obtained from Invitrogen (Auckland, New Zealand). Basic fibroblast growth factor (bFGF) was obtained from Roche Diagnostics NZ Ltd. Milli-Q water was used throughout all studies, and other reagents were of analytical grade.

Cell Culture. RBE4 cells were kindly provided by Professor Michael Aschner (Vanderbilt University, Nashville, TN, USA). The RBE4 medium was a mixture of 50% (v/v) minimum essential medium (alpha medium) and 50% F-10 nutrient mixture supplemented with 10% FBS, 100 U/mL penicillin, 100 μg/mL streptomycin, 2 mM L-glutamine, 1 ng/mL bFGF, and 300 μg/mL Geneticin. Cells were cultured in 75 cm^2 collagen type I coated cell culture flasks (BioCoat, Becton, Dickinson and Company, Auckland, New Zealand) and maintained in a 37 °C incubator with a humidified atmosphere (5% CO_2/95% air). The medium was changed every two days.

Cytotoxicity of Bile Salts. Cytotoxicity of BS to RBE4 cells was measured using the lactate dehydrogenase (LDH) assay. In this assay, the amount of cytoplasmic LDH released into the medium is a measure of the loss of cell membrane integrity. Briefly, aliquots (100 μL) of RBE4 cell suspensions (5×10^5 cells/mL) were added to each well of a 96-well plate and incubated overnight. The cell culture medium was removed, and cells were washed twice with Ringer's-HEPES (RH) buffer (Ringer's buffer containing 10 mM HEPES, pH 7.4). RH buffer (100 μL) containing BS (0.02 −10 mM) was then added to each well. To some wells, RH buffer without BS and 10% Triton X-100 were added in order to obtain LDH background release and maximum release, respectively. After 2 and 24 h incubation, plates were centrifuged at 250g for 4 min, after which 50 μL aliquots of supernatant were transferred to a new 96-well plate and LDH was determined using the LDH CytoTox 96 assay kit (Promega). LDH release was calculated as the percentage of the total LDH activity (the amount of maximum release). The assay was shown to be free of interference from BS.

R123 Uptake Study. In a preliminary study, uptake was shown to reach equilibrium before 2 h such that 2 h was used in all subsequent uptake studies. RBE4 cells were grown in 12-well collagen type I coated multiwell plates (BioCoat) until confluence. After washing three times with prewarmed RH buffer, cells were exposed to 10 or 100 μM R123 in the absence and presence of BS at various concentrations. After 2 h incubation at 37 °C under 5% CO_2/95% air, the incubation was terminated by removing the incubation medium, washing the cells three times with ice-cold PBS and subsequently lysing using 0.5 mL 1% Triton X-100. The fluorescence intensity of R123 in the incubation medium and in the cells was measured using the POLARstar fluorescence microplate reader at excitation and emission wavelengths of 485 and 530 nm, respectively. Intracellular R123 concentration was normalized with respect to total protein content in each well measured using the bicinchoninic acid (BCA) assay (Pierce, Rockford, IL, USA). This involved mixing 25 μL of cell lysate with 200 μL of working reagent and, after 30 min, measuring the absorbance at 562 nm using a plate reader.

In a parallel study, images of the washed cells were captured using a Zeiss LSM 510 inverted confocal microscope (Carl Zeiss Inc., Gottingen, Germany) with full incubation chamber. The plan-Apochromat 10×/0.45 objective was used with 4× zoom function. Image J (National Institutes of Health, USA) image processing and analysis software were used to quantify the cellular uptake of R123.

A similar study was conducted to obtain the extracellular and intracellular R123 concentrations at equilibrium for subsequent mathematical modeling. Cells were exposed to various concentrations of R123 (5–225 μM) in the presence of a fixed concentration of BS (2 mM C and TC; 0.1 mM DC; 5 mM MKC), and after 2 h, the total concentrations of R123 in the extracellular buffer and in the cells were determined.

Modeling R123 Uptake. Some mathematical models have been developed to explore the mechanism of drug transport.[11,12] In this study, a simple mathematical model of R123 uptake was developed based on influx by passive diffusion, transporter-mediated efflux and intracellular binding to proteins and organelles. The mathematical model describes the relationship between the total intracellular concentration of R123 ($C_{in.t}$) and its extracellular concentration (C_{ex}) at equilibrium.

The $C_{in.t}$ was calculated by dividing the mass of R123 in the cells by the cell volume (V_{total}) calculated assuming spherical cells using the equation

$$V_{total} = N \times \frac{4}{3}\pi\left(\frac{d}{2}\right)^3 \quad (1)$$

where N is the number of cells in a well and d is the diameter of a cell. The diameter was determined using Mastersizer S and light microscopy to be 16.8 μm. N was determined using a hemocytometer after which the cell suspension was centrifuged at 1000g for 10 min to obtain a cell pellet. The pellet was lysed using 1% Triton X-100 and the protein concentration of the lysate determined. Combining the results of cell counting and protein concentration, the relationship between cell number and protein concentration was established (294 mg protein is equivalent to 1.66×10^6 cells) to allow N to be calculated from the protein concentration.

The processes involved in R123 transport are shown diagrammatically in Figure 1.

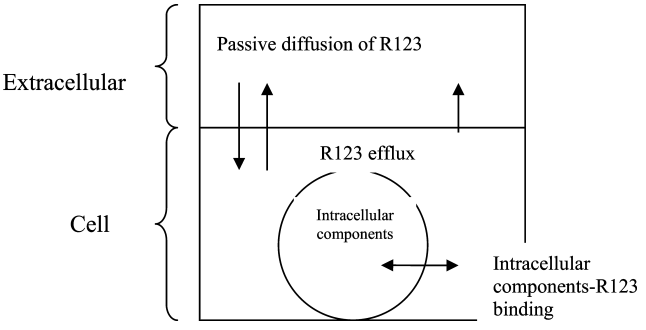

Figure 1. Diagram showing the processes involved in the transport of R123 in RBE4 cells.

At equilibrium, the net flux of R123 across the cell membranes is zero so that influx by passive diffusion equals active efflux:

$$P(C_{ex} - C_{in.f}) = \frac{V_m C_{in.f}}{K_m + C_{in.f}} \quad (2)$$

where P is the passive diffusion rate and $C_{in.f}$ is the intracellular concentration of free R123. The active transporter-mediated efflux is described by a Michaelis–Menten equation[13] where

V_m and K_m are the maximum efflux rate and Michaelis constant of R123 with the transporter.

The total intracellular R123 concentration ($C_{in.t}$) is the sum of the free and bound concentrations. The binding of R123 is described by a saturable binding equation (eq 3) in which B_{max} and K_b are the maximum binding concentration and binding constant of R123 in the cells, respectively.

$$C_{in.t} = C_{in.f} + \frac{B_{max} C_{in.f}}{K_b + C_{in.f}} \quad (3)$$

After rearranging eq 2 and 3, the relationship between C_{ex} and $C_{in.t}$ can be described by eq 4.

$$\begin{aligned} C_{in.t} = {} & 0.5\Big\{ -(V_m/P + K_m - C_{ex}) \\ & + \left[(V_m/P + K_m - C_{ex})^2 + 4C_{ex}K_m\right]^{1/2}\Big\} \\ & + 0.5B_{max}\Big\{ -(V_m/P + K_m - C_{ex}) \\ & + \left[(V_m/P + K_m - C_{ex})^2 + 4C_{ex}K_m\right]^{1/2}\Big\} \\ & \Big/\Big\{K_b + 0.5\Big\{ -(V_m/P + K_m - C_{ex}) \\ & + \left[(V_m/P + K_m - C_{ex})^2 + 4C_{ex}K_m\right]^{1/2}\Big\}\Big\} \end{aligned} \quad (4)$$

Since there is a complete correlation between V_m and P in eq 4, $(V_m)/(P)$ can be replaced by g to give eq 5.

$$\begin{aligned} C_{in.t} = {} & 0.5\Big\{ -(g + K_m - C_{ex}) \\ & + \left[(g + K_m - C_{ex})^2 + 4C_{ex}K_m\right]^{1/2}\Big\} \\ & + \Big\{0.5B_{max}\Big[-(g + K_m - C_{ex}) \\ & + \left[(g + K_m - C_{ex})^2 + 4C_{ex}K_m\right]^{1/2}\Big\} \\ & \Big/\Big\{K_b + 0.5\Big\{ -(g + K_m - C_{ex}) \\ & + \left[(g + K_m - C_{ex})^2 + 4C_{ex}K_m\right]^{1/2}\Big\}\Big\} \end{aligned} \quad (5)$$

The parameters, g, K_m, B_{max} and K_b were estimated by nonlinear regression analysis of $C_{in.t}$ against C_{ex} (Graphpad Prism 5 software, La Jolla, CA, USA). On the assumption that BS do not affect the intracellular binding of R123, B_{max} and K_b were set as global parameters shared by all five data sets (control, C, TC, DC and MKC).

Effect of MKC on R123 Efflux. In this study four groups of RBE4 cells were prepared as follows: cells were loaded with R123 in buffer and subsequently incubated in buffer (buffer−buffer); cells were loaded with R123 in buffer and subsequently incubated in buffer containing MKC (buffer−MKC); cells were loaded with R123 in buffer containing MKC and subsequently incubated in buffer (MKC−buffer); cells were loaded with R123 in buffer containing MKC and subsequently incubated in buffer containing MKC (MKC−MKC). To accomplish this, RBE4 cells were grown in 12-well collagen type I coated multiwall plates until confluent. After washing three times with prewarmed RH buffer, the cells were exposed to 100 μM R123 in RH buffer with and without 1 mM MKC. After 2 h incubation at 37 °C under 5% CO_2/95% air, the R123 solution was aspirated and cells were washed three times with prewarmed RH buffer. Aliquots (1 mL) of prewarmed RH buffer with and without 1 mM MKC were added to some wells and after 15, 30, 60, 90, and 120 min, 0.5 mL aliquots of incubation buffer were removed from these wells and replaced with 0.5 mL prewarmed fresh incubation buffer. After the last sample collection, incubation medium was aspirated, and the cells were washed with ice-cold PBS and lysed with 0.5 mL 1% Triton-X100. The total amount of R123 in RBE4 cells was calculated as the sum of the amount released to the extracellular medium and the amount remaining in the cells after release. The fluorescence intensity of R123 was measured as in the uptake study after ensuring that MKC did not interfere with the fluorescence intensity. The cellular content of R123 was normalized with respect to total protein content measured using the BCA method. The experiment was conducted in triplicate.

Membrane Fluidity. The effect of BS on RBE4 cell membrane fluidity was studied using steady-state fluorescence anisotropy with DPH and TMA-DPH as probes. DPH and TMA-DPH locate in the hydrocarbon core and polar headgroup regions of the lipid bilayer, respectively, such that the magnitude of their fluorescence anisotropy provides information about the fluidity of nonpolar and polar regions of the cell membrane.[14] RBE4 cells grown to confluence were washed three times with RH buffer and then harvested using trypsin-EDTA. Cells were washed and resuspended in RH buffer at a density of 2×10^5 cells/mL after which 1 mM stock solutions of either DPH and TMA-DPH in THF were added to provide a final concentration of 2 μM. After incubation at 37 °C for 1 h in the dark, cell suspensions were centrifuged at 600 g for 3 min and washed twice with RH buffer to remove free probes. BS solutions in RH buffer were then mixed with equal volumes of cell suspension and incubated for 30 min at room temperature in the dark. The fluorescence anisotropy values of DPH or TMA-DPH labeled RBE4 cells were measured using a POLARstar fluorescence microplate reader (BMG Laboratories, Germany) with excitation and emission wavelengths of 350 and 420 nm, respectively. Fluorescence anisotropy (r) is expressed as

$$r = \frac{I_{\parallel} - I_{\perp}}{I_{\parallel} + 2I_{\perp}} \quad (6)$$

where $I_{\parallel}$ is the fluorescence intensity parallel to the excitation plane and $I_{\perp}$ is the fluorescence intensity perpendicular to the excitation plane.

Distribution of R123 in a Liposome/Buffer System. The apparent distribution coefficient of R123 $D_{lip/buffer}$ in the absence and presence of BS was studied in a unilamellar DPPC liposome/buffer system using capillary electrophoresis-frontal analysis (CE-FA) as described previously.[15,16]

Bile Salt/R123 Binding. The binding constants between BS and R123 were determined by mobility shift affinity capillary electrophoresis as described previously.[15]

Statistical Analysis. Data were analyzed by one-way ANOVA with Tukey's or Dunnett's post hoc tests depending on the results of homogeneity of variance tests for multiple

comparisons with SPSS 11.0 (Systat Software Inc., San Jose, CA). Differences for which $p < 0.05$ were considered significant. GraphPad Prism 5 was used for fitting nonlinear regression models.

RESULTS

Cytotoxicity of Bile Salts. The four BS showed different cytotoxicities to RBE4 cells; DC caused the greatest cytotoxicity whereas TC was nontoxic even at 10 mM (Figure 2). MKC showed time-dependent toxicity being virtually nontoxic after 2 h incubation (Figure 2A) but causing 100% leakage of LDH at a concentration of 5 mM after 24 h (Figure 2B). The order of cytotoxicity of BS toward RBE4 cells was TC < MKC < C < DC.

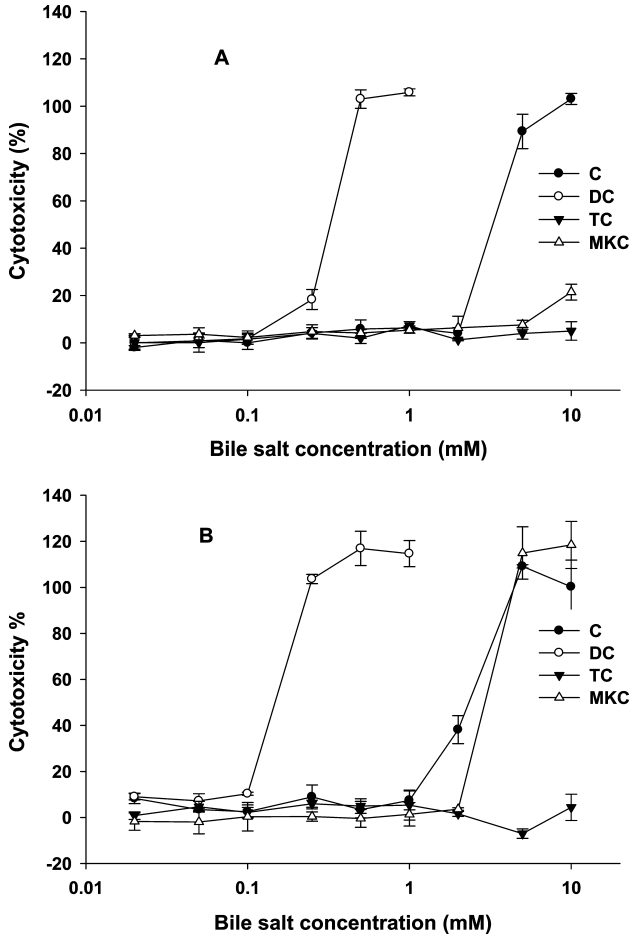

Figure 2. Cytotoxicity of bile salts to RBE4 cells as measured using the LDH assay: (A) after 2 h and (B) after 24 h incubation (data are means ± SD, $n = 4$).

R123 Uptake Study. At 10 μM R123, C, DC and TC had no significant effect on R123 uptake whereas MKC caused a large concentration-dependent increase in R123 uptake up to 2 mM (Figure 3A). At 100 μM R123, C, DC and MKC showed concentration-dependent increases in R123 uptake with MKC having the greatest effect (Figure 3B). In the case of TC, R123 uptake decreased significantly above 2 mM; this is possibly the result of the incorporation of R123 into TC micelles since, in contrast to the other BS, the higher concentrations of TC exceed its CMC (3.6 mM[6]).

These changes or lack thereof were supported by confocal micrographs of RBE4 cells after 2 h incubation with either 10 or 100 μM R123 in the absence and presence of BS (Figure 4). At 10 μM R123, fluorescence intensities of the control, C, TC and DC treated groups were similar but fluorescence was much greater in the MKC group indicating increased R123 uptake. At 100 μM R123, MKC again showed the greatest increase in fluorescence intensity. It was found that the fluorescence intensity was evenly distributed along the z-axis, suggesting R123 is inside the cells.

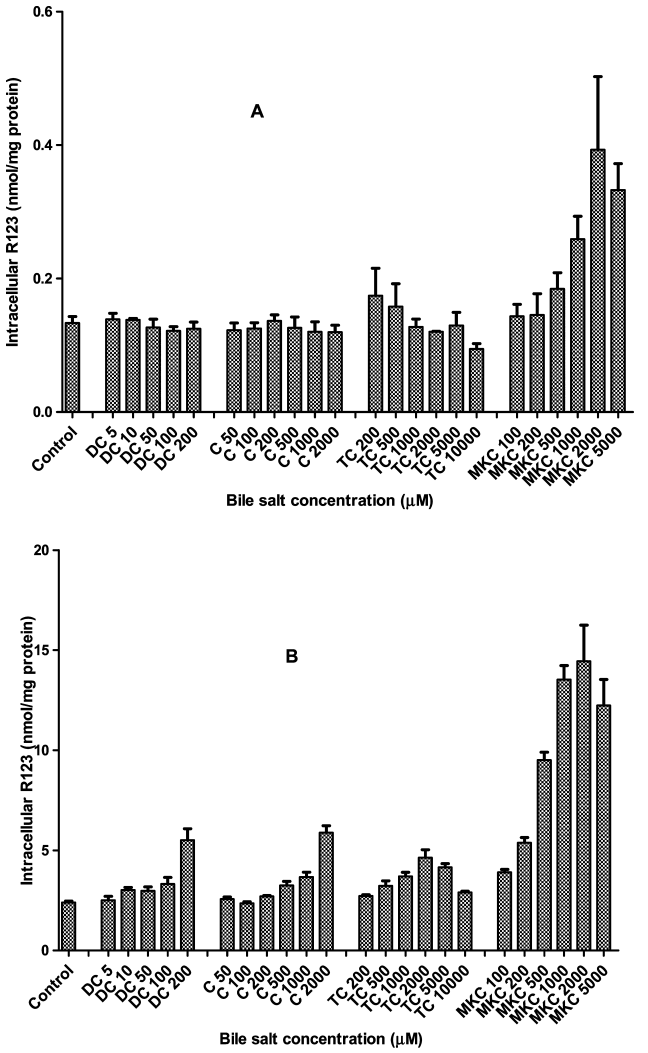

Figure 3. Effect of bile salts on R123 uptake into RBE4 cells after 2 h at R123 loading concentrations of (A) 10 μM and (B) 100 μM (data are means ± SD, $n = 4$).

Modeling R123 Uptake. The results of the estimation of g (V_m/P) and K_m using the mechanistic model (eq 5) are shown in Figure 5 and Table 1. The model gave good fits to the data as judged by the randomness of the residuals and the fact that in all cases $R^2 > 0.927$. When simple protein binding was not included in the model, the fit was not as good based on the Akaike Information Criterion.[17] Starting estimates for the parameters were varied over a wide range to test whether the program was converging to a global minimum. Irrespective of the starting value, the program converged to the same final values, giving confidence that the global minimum was found. C and TC showed no effect on R123 uptake compared to control over the concentration range studied. In contrast, MKC and DC caused a significant increase in R123 uptake but by apparently different mechanisms given the different shapes of

dx.doi.org/10.1021/mp200201y | Mol. Pharmaceutics 2012, 9, 29–36

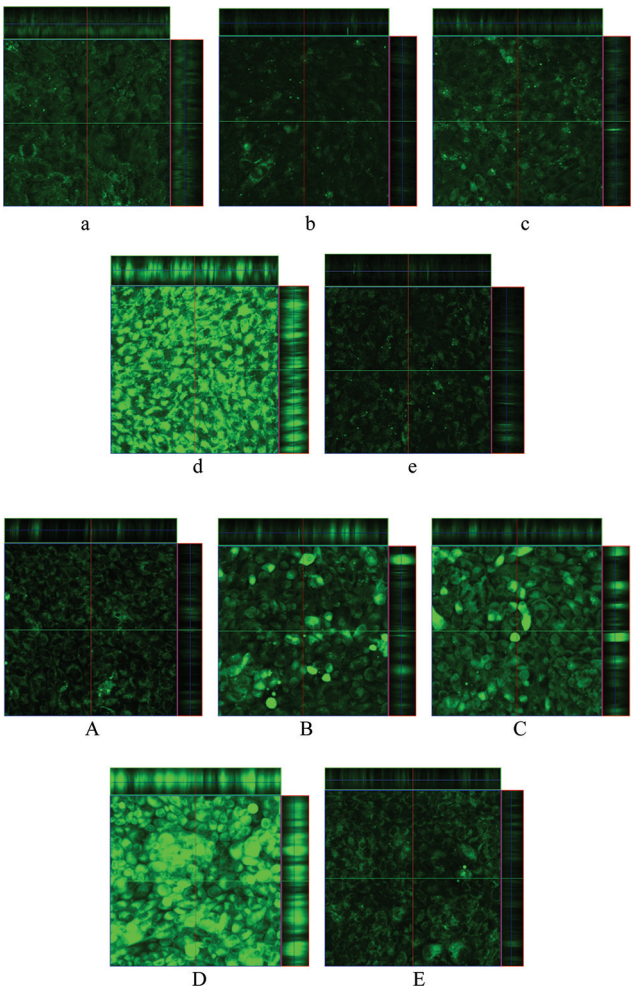

Figure 4. Gallery-view micrographs of three orthogonal sections of RBE4 cells obtained by confocal laser scanning microscopy. Images acquired after 2 h incubation of RBE4 cells with 10 μM R123 (a) in the absence and (b–e) in the presence of bile salts (b, 1 mM C; c, 0.2 mM DC; d, 1 mM MKC; e, 1 mM TC) and with 100 μM R123 (A) in the absence and (B–E) in the presence of bile salts (B, 1 mM C; C, 0.2 mM DC; D, 1 mM MKC; E, 1 mM TC). The small bright dots in the images are probably due to R123 in mitochondria.

the fits (Figure 5). The resulting lower values of g for MKC and DC (Table 1) are due to a reduction in V_m and/or an increase in P. The K_m value of DC was less than those of the other BS, but the differences were not significant.

Effect of MKC on R123 Efflux from Preloaded Cells. Consistent with the equilibrium uptake results (Figure 3B), the presence of 1 mM MKC in the loading buffer significantly enhanced R123 uptake from 2 to 10 nmol/mg protein. Nevertheless, the total intracellular concentrations of R123 were found to be equal in the buffer–buffer and buffer–MKC groups and were also equal in the MKC–buffer and MKC–MKC groups (data not shown).

The time course for the release of R123 from RBE4 cells preloaded with R123 in the absence and presence of MKC is shown in Figure 6. After 2 h, the release of R123 from cells in the buffer–buffer group approached 100% whereas that from those in the buffer–MKC group was about 80%. The initial rate of release of R123 from cells in the buffer–MKC group is similar to that from cells in the buffer–buffer group but the rate subsequently decreases such that after 20 min the amount

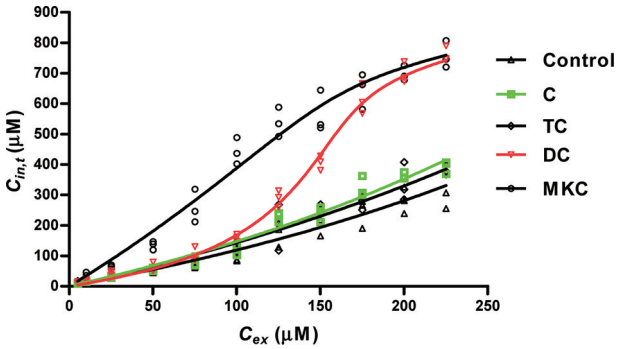

Figure 5. Effect of bile salts (2 mM for C and TC; 0.1 mM for DC and 5 mM for MKC) on R123 uptake at various R123 concentrations into RBE4 cells after 2 h incubation. The lines are nonlinear regression lines of the total intracellular R123 concentration ($C_{in,t}$) against the extracellular R123 concentration (C_{ex}) for R123 uptake in the presence of bile salts using eq 5.

Table 1. Effect of a Fixed Concentration of Bile Salts on R123 Uptake into RBE4 Cells[a]

params (μM)	control	2 mM C	2 mM TC	5 mM MKC	0.1 mM DC
g (V_m/P)	361 ± 19	314 ± 8	341 ± 13	161 ± 6	163 ± 3
K_m	2.6 ± 0.9	2.8 ± 0.8	3.0 ± 0.9	3.8 ± 1.7	1.0 + 0.2
B_{max}[b]	732	732	732	732	732
K_b[b]	5.21	5.21	5.21	5.21	5.21
R^2	0.927	0.980	0.955	0.981	0.992

[a]Parameters estimated using nonlinear regression of $C_{in,t}$ against C_{ex} in eq 5 (data are means ± SE) with coefficients of determination (R^2) for each regression line. [b]Estimated globally across all data sets.

effluxed is significantly lower than in the buffer–buffer group. In the MKC–buffer and MKC–MKC groups, there was no difference in the rate of release over the first 30 min but, thereafter, the MKC–buffer group showed a much faster rate of release than that from the MKC–MKC group. After 2 h, nearly 100% of R123 was released from cells in the MKC–buffer group but only 60% from those in the MKC–MKC group.

Membrane Fluidity. Changes in fluorescence anisotropy are inversely related to membrane fluidity. Decreases in fluorescence anisotropy of both DPH and TMA-DPH occurred on exposure to BS (Figure 7), suggesting BS increase membrane fluidity. There was little difference in the effect of BS on the fluorescence anisotropy of DPH, but there were significant differences in their effects on the fluorescence anisotropy of TMA-DPH.

Effect of Bile Salts on R123 Liposome/Buffer Distribution Coefficients. BS significantly increased the apparent $D_{lip/buffer}$ of R123 in a concentration-dependent manner (Figure 8). DC increased it to the greatest extent, with C and TC increasing it less and to similar extents. MKC showed the least effect on the apparent $D_{lip/buffer}$ of R123.

Bile Salt/R123 Binding. All BS were found to bind to R123 with low binding constants (K). The percentage bound (F) in the presence of all BS was low (Table 2).

DISCUSSION

Cytotoxicity of BS usually correlates with their lipophilicity[18–20] which, in the liposome/buffer system, was found to be in the order MKC < TC ≈ C < DC (Yang et al., unpublished data). With the exception of TC, this is also the order of increasing cytotoxicity to RBE4 cells (Figure 2). The noticeable

dx.doi.org/10.1021/mp200201y | Mol. Pharmaceutics 2012, 9, 29–36

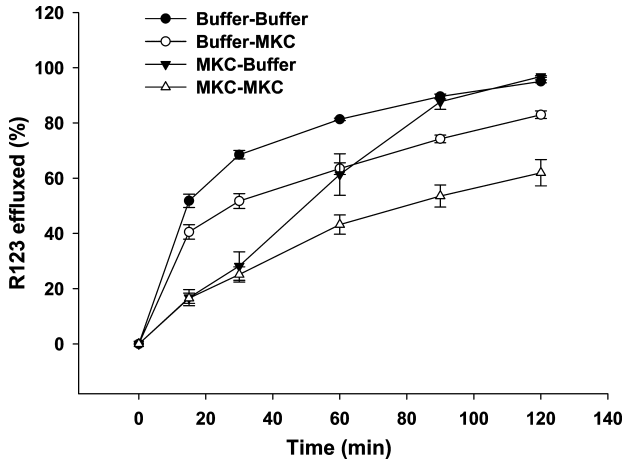

Figure 6. Effect of MKC on the release of R123 from RBE4 cells preloaded with R123 in the absence and presence of MKC. Buffer–buffer: buffer in loading and release media. Buffer–MKC: buffer in loading medium and MKC in release medium. MKC–buffer: MKC in loading medium and buffer only in release medium. MKC–MKC: MKC in both loading and release media (data are means ± SD, n = 3).

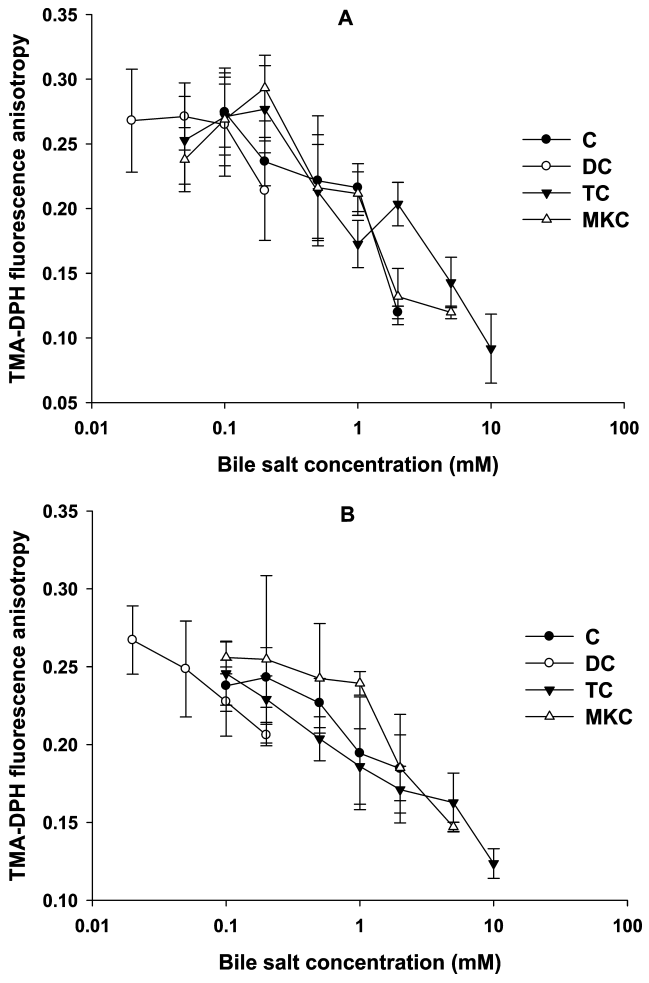

Figure 7. Effect of bile salts on the fluorescence anisotropy of (A) DPH and (B) TMA-DPH in RBE4 cells (data are means ± SD, n = 4).

absence of cytotoxicity of TC may reflect the presence of a specific efflux transport system for TC in RBE4 cells, a possibility supported by the fact that TC is effluxed from the brain to the circulating blood via a specific mechanism.[21]

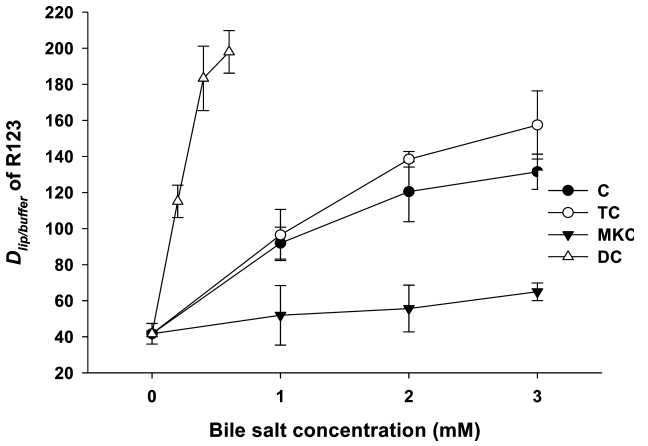

Figure 8. Effect of bile salt concentration on the apparent distribution coefficient of R123 ($D_{lip/buffer}$) in the DPPC liposome/buffer system (2 mM lipid, Ringer's-HEPES buffer at pH 7.4). (Data are means ± SD, n = 3.)

Table 2. Binding Constants (K) and Percentage Bound (F) between Bile Salts and R123 in Ringer's-HEPES Buffer at pH 7.4[a]

	C	DC	MKC	TC
K (M^{-1})	34.6 ± 2.0	74.0 ± 7.2	63.8 ± 5.0	33.1 ± 3.3
F[b] (%)	3.3	6.9	6.0	3.2

[a]Data are means ± SD, n = 3. [b]Determined using 50 μM R123 and 1 mM bile salt.

R123 is a well-known P-gp substrate which is frequently used to examine P-gp activity in cell culture models[8] and to test whether a drug is a P-gp inhibitor or substrate.[22,23] Recent studies indicate that R123 is also a substrate of multidrug resistance-associated proteins (MRPs), specifically MRP1.[24] MRP1 is expressed in RBE4 cells but is probably not functional given that probenecid, an MRP inhibitor, does not affect the accumulation of vincristine, an MRP1 substrate, in RBE4 cells.[25] On this basis, intracellular accumulation of R123 in RBE4 cells can be considered to result from a competition between its passive influx and P-gp efflux.

At the lower loading concentration of R123 (10 μM) where P-gp efflux is expected to have a greater influence, only MKC significantly increased R123 uptake by RBE4 cells (Figure 3A). At the higher loading concentration of R123 (100 μM) where P-gp is expected to be saturated (the half-saturation concentration of R123 for P-gp efflux has been shown to be 7.2 μM in K562 cells[26] and 13.5 μM in plasma membrane vesicles[27]), all BS increased R123 uptake with MKC having the greatest effect. These results are consistent with MKC inhibiting P-gp and/or enhancing passive diffusion of R123.

Using the mathematical model to explore the effect of BS on R123 uptake, it was found that MKC and DC significantly decreased the value of V_m/P, indicating they decrease V_m of R123 efflux and/or increase P of R123 (Table 1). Figure 5 shows that MKC and DC produce different regression profiles, suggesting they affect uptake by different mechanisms. At low C_{ex}, only MKC increases R123 uptake ($C_{in,t}$) compared to control whereas, at high C_{ex}, both MKC and DC increase R123 uptake compared to control. At low C_{ex}, efflux by P-gp should predominate so that the increased uptake of R123 in the presence of MKC is probably due to its ability to inhibit the

dx.doi.org/10.1021/mp200201y | Mol. Pharmaceutics 2012, 9, 29–36

kinetic process of P-gp efflux (V_m). At high C_{ex}, the increase in R123 uptake in the presence of DC can be explained by its ability to increase passive diffusion (P). However, a synergistic cytotoxicity of R123 and DC causing a fall in the V_m of P-gp could also explain the results for DC, and this cannot be ruled out.

In the studies of R123 efflux from RBE4 cells, P-gp efflux is superimposed on passive efflux down the concentration gradient. The fact that cells in the buffer−buffer group released R123 more rapidly than cells in the buffer−MKC group is consistent with inhibition of P-gp by MKC (Figure 6). The slower but equal initial rate of release from cells in the MKC−buffer and MKC−MKC groups is consistent with more efficient inhibition of P-gp by the preloaded MKC. The subsequently faster release from cells in the MKC−buffer group probably reflects recovery of P-gp as MKC leaks out of the cells.

Previously, it has been shown that C, DC and TC do not affect P-gp function in both multidrug resistant cells and rat canalicular membrane vesicles whereas taurolithocholate (TLCA), taurochenodeoxycholate (TCDC), glycochenodeoxycholate (GCDC) and ursodeoxycholate (UDC) inhibit P-gp mediated drug transport in both systems.[28] Although TLCA, TCDC, GCDC and UDC have different chemical structures, they all share with MKC the absence of a hydroxyl group at position 12, suggesting this is a crucial structural feature for BS to inhibit P-gp.

With regard to the mechanism by which MKC inhibits P-gp, it must occur either through an interaction with the surrounding cell membrane or by interaction with P-gp itself. The fact that MKC is the least hydrophobic and least membrane fluidizing of the four BS tends to suggest MKC inhibition of P-gp is not mediated through an increase in membrane fluidity. Rather it may be that MKC or water brought into the membrane in association with MKC[29] interacts with P-gp by hydrogen bond formation within the lipid membrane. This would indicate that, of all the BS tested, MKC is able to take up a conformation with a particularly favorable hydrogen bonding pattern due to the presence of its ketone hydrogen bond acceptor group.

The results of the membrane fluidity study (Figure 7) suggest that BS increase membrane fluidity in both the hydrophobic core and polar surface regions of the lipid bilayer. This increase in membrane fluidity leading to an increase in the passive diffusion of R123 is one explanation for the increases in R123 uptake produced by C, DC and TC (up to 2 mM) at the higher R123 concentration (Figure 3). Other possible explanations are that BS increase the negativity of the RBE4 cell membrane to facilitate partitioning of cationic R123 into cell membranes and that anionic bile salts form ion pairs with cationic R123 (Table 2) to increase its apparent lipophilicity. The former is supported by the fact that BS increase the zeta potential of DPPC liposomes[16] whereas the latter is unlikely to make a significant contribution given that the BS-R123 binding constants (Table 2) are not very high.

■ CONCLUSION

C, DC, MKC and TC differ in their ability to enhance R123 uptake into RBE4 cells. The mechanistic studies suggest that bile salts increase R123 uptake via modulating membrane fluidity and surface charge. The contribution from ion pair formation between anionic bile salts and cationic R123 appears to be small. MKC differs from the other three bile salts in that it significantly inhibits the efflux of R123 by P-gp, probably by affecting the kinetic process of efflux.

■ AUTHOR INFORMATION

Corresponding Author

*School of Pharmacy, University of Otago P.O. Box 56, Dunedin 9054, New Zealand. Office phone: +64 3 4799033. Cell phone: +64 221780602. Fax: + 64 3 4797034. E-mail: lin.yang@otago.ac.nz.

■ ACKNOWLEDGMENTS

The authors gratefully acknowledge financial support from the New Zealand Pharmacy Education and Research Foundation (Grant No. 160OU). L.Y. also thanks the Drug Research Academy, Faculty of Pharmaceutical Sciences, University of Copenhagen for providing financial assistance and the University of Otago for providing a Postgraduate Publishing Bursary.

■ REFERENCES

(1) Mukaizawa, F.; Taniguchi, K.; Miyake, M.; Ogawara, K. i.; Odomi, M.; Higaki, K.; Kimura, T. Novel oral absorption system containing polyamines and bile salts enhances drug transport via both transcellular and paracellular pathways across Caco-2 cell monolayers. *Int. J. Pharm.* **2009**, *367* (1−2), 103−108.

(2) Meaney, C. M.; O'Driscoll, C. M. A comparison of the permeation enhancement potential of simple bile salt and mixed bile salt:fatty acid micellar systems using the CaCo-2 cell culture model. *Int. J. Pharm.* **2000**, *207* (1−2), 21−30.

(3) Mikov, M.; Kevresan, S.; Kuhajda, K.; Jakovljevic, V.; Vasovic, V. 3Alpha,7alpha-dihydroxy-12-oxo-5beta-cholanate as blood-brain barrier permeator. *Pol. J. Pharmacol.* **2004**, *56* (3), 367−371.

(4) Vasovic, V.; Vukmirovic, S.; Pjevic, M.; Mikov, I.; Mikov, M.; Jakovljevic, V. Influence of bile acid derivates on tramadol analgesic effect in mice. *Eur. J. Drug Metab. Pharmacokinet.* **2010**, *35* (1−2), 75−78.

(5) Kuhajda, I.; Poša, M.; Jakovljević, V.; Ivetić, V.; Mikov, M. Effect of 12-monoketocholic acid on modulation of analgesic action of morphine and tramadol. *Eur. J. Drug Metab. Pharmacokinet.* **2009**, *34* (2), 73−78.

(6) Yang, L.; Zhang, H.; Mikov, M.; Tucker, I. G. Physicochemical and biological characterization of monoketocholic acid, a novel permeability enhancer. *Mol. Pharmaceutics* **2009**, *6* (2), 448−456.

(7) Yang, L.; Zhang, H.; Fawcett, J. P.; Mikov, M.; Tucker, I. G. Effect of bile salts on the transport of morphine-6-glucuronide in rat brain endothelial cells. *J. Pharm. Sci.* **2011**, *100* (4), 1516−1524.

(8) Fontaine, M.; Elmquist, W. F.; Miller, D. W. Use of rhodamine 123 to examine the functional activity of P-glycoprotein in primary cultured brain microvessel endothelial cell monolayers. *Life Sci.* **1996**, *59* (18), 1521−1531.

(9) Altenberg, G. A.; Vanoye, C. G.; Horton, J. K.; Reuss, L. Unidirectional fluxes of rhodamine 123 in multidrug-resistant cells: Evidence against direct drug extrusion from the plasma membrane. *Proc. Natl. Acad. Sci. U.S.A.* **1994**, *91* (11), 4654−4657.

(10) Neyfakh, A. A. Use of fluorescent dyes as molecular probes for the study of multidrug resistance. *Exp. Cell Res.* **1988**, *174* (1), 168−176.

(11) Jang, S. H.; Guillaume Wientjes, M.; Au, J. L. S. Kinetics of P-glycoprotein-mediated efflux of paclitaxel. *J. Pharmacol. Exp. Ther.* **2001**, *298* (3), 1236−1242.

(12) Kuh, H. J.; Jang, S. H.; Wientjes, M. G.; Au, J. L. S. Computational model of intracellular pharmacokinetics of paclitaxel. *J. Pharmacol. Exp. Ther.* **2000**, *293* (3), 761−770.

(13) Sugano, K.; Kansy, M.; Artursson, P.; Avdeef, A.; Bendels, S.; Di, L.; Ecker, G. F.; Faller, B.; Fischer, H.; Gerebtzoff, G.; Lennernaes, H.; Senner, F. Coexistence of passive and carrier-mediated processes in drug transport. *Nat. Rev. Drug Discovery* **2010**, *9* (8), 597−614.

(14) Kuhry, J. G.; Fonteneau, P.; Duportail, G.; Maechling, C.; Laustriat, G. TMA-DPH: A suitable fluorescence polarization probe

for specific plasma membrane fluidity studies in intact living cells. *Cell Biophys.* **1983**, *5* (2), 129−140.
(15) Yang, L.; Tucker, I. G.; Østergaard, J. Effects of bile salts on propranolol distribution into liposomes studied by capillary electrophoresis. *J. Pharm. Biomed. Anal.* **2011**, *56* (3), 553−559.
(16) Franzen, U.; Jorgensen, L.; Larsen, C.; Heegaard, N. H. H.; Østergaard, J. Determination of liposome-buffer distribution coefficients of charged drugs by capillary electrophoresis frontal analysis. *Electrophoresis* **2009**, *30* (15), 2711−2719.
(17) Motulsky, H.; Christopoulos, A. *Fitting Models to Biological Data Using Linear and Nonlinear Regression: A Practical Guide to Curve Fitting*; GraphPad Software, Inc.: San Diego, 2003.
(18) Delzenne, N. M.; Calderon, P. B.; Taper, H. S.; Roberfroid, M. B. Comparative hepatotoxicity of cholic acid, deoxycholic acid and lithocholic acid in the rat: in vivo and in vitro studies. *Toxicol. Lett.* **1992**, *61* (2−3), 291−304.
(19) Sagawa, H.; Tazuma, S.; Kajiyama, G. Protection against hydrophobic bile salt-induced cell membrane damage by liposomes and hydrophilic bile salts. *Am. J. Physiol.* **1993**, *264* (5 Pt 1), G835−G839.
(20) Benedetti, A.; Alvaro, D.; Bassotti, C.; Gigliozzi, A.; Ferretti, G.; Rosa, T. L.; Sario, A. D.; Baiocchi, L.; Jezequel, A. M. Cytotoxicity of bile salts against biliary epithelium: A study in isolated bile ductule fragments and isolated perfused rat liver. *Hepatology* **1997**, *26* (1), 9−21.
(21) Kitazawa, T.; Terasaki, T.; Suzuki, H.; Kakee, A.; Sugiyama, Y. Efflux of taurocholic acid across the blood-brain barrier: interaction with cyclic peptides. *J. Pharmacol. Exp. Ther.* **1998**, *286* (2), 890−895.
(22) Dintaman, J. M.; Silverman, J. A. Inhibition of P-glycoprotein by D-alpha-tocopheryl polyethylene glycol 1000 succinate (TPGS). *Pharm. Res.* **1999**, *16* (10), 1550−1556.
(23) Kim, A. E.; Dintaman, J. M.; Waddell, D. S.; Silverman, J. A. Saquinavir, an HIV protease inhibitor, is transported by P-glycoprotein. *J. Pharmacol. Exp. Ther.* **1998**, *286* (3), 1439−1445.
(24) Daoud, R.; Kast, C.; Gros, P.; Georges, E. Rhodamine 123 binds to multiple sites in the multidrug resistance protein (MRP1). *Biochemistry* **2000**, *39* (50), 15344−15352.
(25) Regina, A.; Koman, A.; Piciotti, M.; El Hafny, B.; Center, M. S.; Bergmann, R.; Couraud, P. O.; Roux, F. Mrp1 multidrug resistance-associated protein and P-glycoprotein expression in rat brain microvessel endothelial cells. *J. Neurochem.* **1998**, *71* (2), 705−715.
(26) Wang, Y.; Hao, D.; Stein, W. D.; Yang, L. A kinetic study of Rhodamine123 pumping by P-glycoprotein. *Biochim. Biophys. Acta, Biomembr.* **2006**, *1758* (10), 1671−1676.
(27) Adam, B. S.; Victor, L. Positively cooperative sites for drug transport by P-glycoprotein with distinct drug specificities. *Eur. J. Biochem.* **1997**, *250* (1), 130−137.
(28) Roberto, M.; Ornella, F.; Yukkio, K.; Zenaida, G.; Paolo, G.; Irwin, M. A. Bile acid inhibition of P-glycoprotein-mediated transport in multidrug-resistant cells and rat liver canalicular membrane vesicles. *Hepatology* **1994**, *20* (1), 170−176.
(29) Mohapatra, M.; Mishra, A. K. 1-Naphthol as a sensitive fluorescent molecular probe for monitoring the interaction of submicellar concentration of bile salt with a bilayer membrane of DPPC, a lung surfactant. *J. Phys. Chem. B* **2010**, *114* (46), 14934−14940.